Laser and Particle Beams (2011), *29*, 29–37.
© Cambridge University Press, 2010 0263-0346/11 $20.00
doi:10.1017/S0263034610000728

Protons and ion acceleration from thick targets at 10^{10} W/cm^2 laser pulse intensity

L. TORRISI,[1] F. CARIDI,[2] AND L. GIUFFRIDA[3]

[1]Dipartimento di Fisica, Messina, Italy and INFN-Laboratori Nazionali del Sud, Catania, Italy
[2]Facoltà di Scienze MM.FF.NN., Università di Messina, Messina, Italy and INFN-Sez. CT, Gruppo Collegato di Messina, Messina, Italy
[3]Dipartimento di Fisica, Messina, Italy and INFN-Laboratori Nazionali del Sud, Catania, Italy

(RECEIVED 1 May 2010; ACCEPTED 15 October 2010)

Abstract

Proton ion acceleration *via* laser-generated plasma is investigated at relatively low laser pulse intensity, on the order of 10^{10} W/cm^2. Time-of-flight technique is employed to measure the ion energy and the relative yield. An ion collector and an ion energy analyzer are used with this aim and to distinguish the number of charge states of the produced ions. The kinetic energy and the emission yield are measured through a consolidated theory, which assumes that the ion emission follows the Coulomb-Boltzmann-Shifted function. The proton stream is generated by thin and thick hydrogenated targets and it is dependent on the free electron states, which increase the laser absorption coefficient and the ion acceleration. The maximum proton energy, of about 200 eV, and the maximum proton amount can be obtained with thick metallic hydrogenated materials, such as the titanium hydrate TiH_2.

Keywords: Coulomb-Boltzmann-shifted distribution; Laser-generated plasma; Metal ablation; Polymer ablation

1. INTRODUCTION

The ion acceleration from thick targets irradiated by low energy pulsed lasers is a research field several investigated in the last years. However, the proton acceleration has been less considered in this regime due to the difficulty to detect the low energetic protons, to measure the proton energy distribution, and to analyze the low proton amount involved in the plasma acceleration process.

The total kinetic energy conferred to the plasma ions ejected along the normal to the target surface is due to thermal and Coulomb interactions. The first contribution takes into account the plasma temperature and the adiabatic plasma expansion in vacuum. The second contribution is due to the development of a fast electron cloud emission from the target and to a consequent Coulomb explosion effect occurring in the atomic surface structure. Ions are emitted slowly with respect to electrons and a charge space separation between fast electrons and slower ions is produced near the target surface for a time value comparable with the laser pulse duration. This process generates a high electric field due to charge separation at a distance comparable with the Debye length, on the order of MV/cm, directed along the normal to the target surface. This electric field is responsible of the high acceleration of the ions dependently on their charge state, of the low emissivity of the ion beam, and of the energetic shift of the ions Boltzmann distributions.

The advantage to use low laser intensity, on the order of 10^{10} W/cm^2, consists with the low cost of the laser system, and the possibility to use high repetition rates hitting roto-translating thick targets. This operation method permits to generate high ion plasma current, emitted with low energy, Boltzmann distributions, and low emittance along the normal to the target surface. Laser ion-sources, intense visible and ultraviolet sources, generation of multi-energetic ion beams, represent some of the different possible applications in the field of ion accelerator, intense photon sources, ion sputtering, and ion implantation fields. Protons and ions emitted from plasma, for example, can be submitted to a post acceleration voltage to be accelerated up to energies on the order of 100–1000 keV (Torrisi *et al.*, 2010). Moreover, the investigations at low laser intensities can be employed to develop a research on the target composition and geometry, preliminary to the use of higher laser intensities in order to accelerate ions at high energy and current. In

Address correspondence and reprint requests to: Francesco Caridi, Facoltà di Scienze MM.FF.NN., Università di Messina, Ctr. Papardo 31, 98166, Messina, Italy. E-mail: fcaridi@unime.it

https://doi.org/10.1017/S0263034610000728 Published online by Cambridge University Press

particular, a relevant interest is actually devoted to hydrogenated targets able to generate a large amount of protons with high kinetic energy and narrow angular distribution. The use of polymers, polymer/metal multilayer films, and nanostructures embedded in polymers, for example, promotes high resonant absorption effects with high photon energy transfer to the protons (Badziak *et al.*, 2008).

Spatial and spectral distributions of plasma-generated ions don't represent an obstacle to their applicability. For applications in the field of surface treatment of ion sputtering and ion implantation, for example, the use of multi ion species and of multi ion energies permits to treat contemporary different surface layers and, at high dose, to modify their chemical and physical properties. Moreover, the emitted ions from the target can be focused using external magnetic fields directed orthogonally to the target surface and the produced ion beam can reach dimensions on the order of 10 mm^2.

Generally, proton energies remain below 100 eV at laser intensities on the order of 10^{10} W/cm^2 or less. However, the use of a post-ion acceleration process may permit to increase the ion energy proportionally to the applied acceleration voltage, and to the ion charge state. Moreover, the use of a suitable magnetic field permits to focus the ion beam and to increase its emittance (Torrisi *et al.*, 2007). The ion and proton detection based on time-of-flight (TOF) technique remains a simple but very efficient method to investigate the ion stream emission from the fast non-equilibrium plasma produced by a laser shot, as will be demonstrated in this article.

Laser-generated plasma contains ions with kinetic energy proportionally to the $I\lambda^2$, where I is the laser intensity and λ is the laser wavelength (Laska *et al.*, 2005). Thus, at low laser intensities, such as that used in this experiment, the expected energies should be very low, while at high intensities, above 10^{19} W/cm^2 obtainable with ultra-fast fs lasers, the proton energy may assume values of the order of tens MeV (Clark *et al.*, 2000).

The special interest for protons production by plasma laser, and also for other light ions such as carbon, in terms of energy and yield and of fast repetitive streams, derives from the applications that energetic ion beams can have without the use of expensive and large ion accelerators. The new generation of ion sources, the nuclear physics, the astrophysics, the medicine, the chemistry, and the nuclear fusion researches are strongly interested to this theme also if relatively low laser pulse intensity is employed.

2. MATERIALS AND METHODS

A *Q*-switched Nd:Yag pulsed laser operating at 1064 nm fundamental wavelength, with 9 ns pulse duration and 1 to 900 mJ pulse energy, in single laser shot mode (operating also at 1–10 Hz repetition rate), is employed for this experiment.

The laser beam is focused, through a 50 cm focal lens placed in air, on the surface of a thick (1–2 mm) target placed inside a vacuum chamber at 10^{-6} mbar. The laser light passes through a thin glass window to the target, on which it produces a 0.5 mm^2 spot size.

The laser intensity on the target was measured through the joule-meter and the laser spot dimension measurements. This last one was determined by the analysis of the produced craters with a surface profiler (Tencor P-10) having a depth resolution of 10 nm and a lateral resolution of 0.05 mm.

The employed targets are hydrogenated materials, in order to produce high proton emission. The investigated target were: polyethylene (CH_2), bulk metals (Al, Ti, Au) covered by thin (10–50 μm thickness) polyethylene films, titanium hydride TiH_2, and titanium with absorbed hydrogen $Ti(H_2)$. The target is mounted on a holder (externally vertically and angularly mobile) at an incident angle of 30°. A photo and a scheme of the experimental setup are reported in Figures 1a and 1b, respectively.

An ion collector (IC) placed horizontally along the normal to the target surface and generally at 60 cm distance from the target surface, is used in TOF approach (Woryna *et al.*, 1996). An electrostatic ion energy analyzer (IEA) permits to measure the energy-to-charge ratio through the ion deflection and to know the number of charge states of the plasma

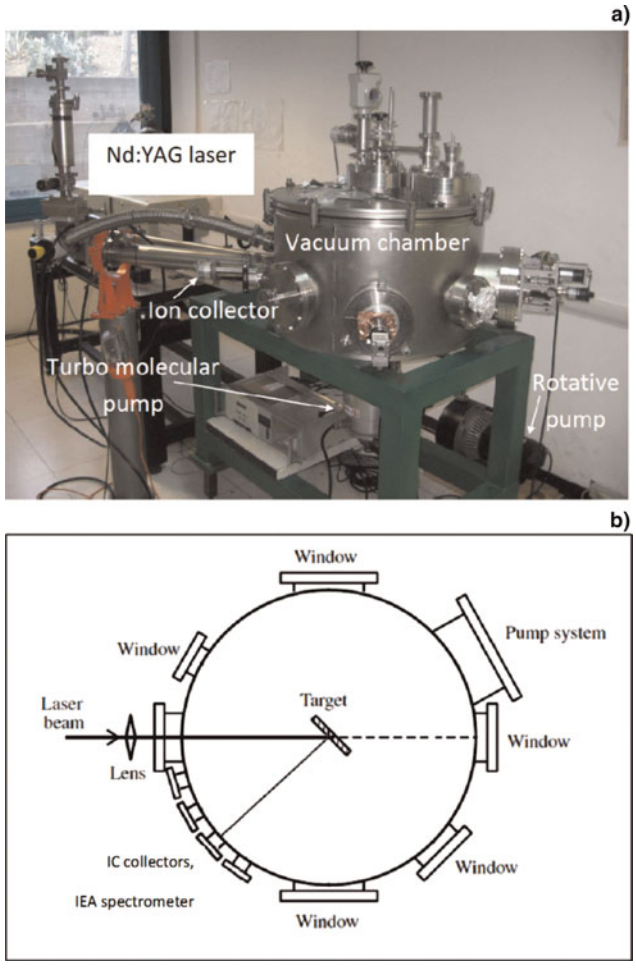

Fig. 1. (Color online) A photo (**a**) and a scheme (**b**) of the experimental setup.

https://doi.org/10.1017/S0263034610000728 Published online by Cambridge University Press

ions (Torrisi *et al.*, 2008). The IEA detector was placed at 160 cm from the target.

All IC and IEA analyses presented in this paper are obtained by a single laser shot given to fresh surface. No data are presented for multiple repeated shots in the same target place.

The Coulomb-Boltzmann-Shifted (CBS) function was employed to deconvolve the experimental ion spectra in the different ion species and charge state contributions (Torrisi *et al.*, 2002). The experimental IC spectra, recorded with a fast storage oscilloscope and represented in terms of ion time distributions, follow the CBS relationship:

$$F(t) = A \cdot \left(\frac{m}{2\pi kT}\right)^{3/2} \cdot \left(\frac{L^4}{t^5}\right) \times \exp\left[-\left(\frac{m}{2kT}\right)\left(\frac{L}{t} - \sqrt{\frac{\gamma kT}{m}} - \sqrt{\frac{2zeV_0}{m}}\right)^2\right] \quad (1)$$

where m is the ion mass, kT is the equivalent temperature (in eV), L is the target-IC detector distance, γ is the adiabatic coefficient, ze is the ion charge, and $V0$ is the equivalent acceleration voltage developed in the non-equilibrium plasma (Caridi *et al.,* 2010).

IC and IEA detectors give only relative information on the ions collected along their subtended solid angle. In particular IEA permits to measure with high precision the ion energy, the ion charge states and the energy-to-charge state, E/z, ratio of the detected species for a given deflection bias. By varying the deflection voltage it is possible to evaluate the ion energy distributions as a function of the ion charge state. Consequently, it is possible to compare the ion yields as a function of the charge states. On the base of the IEA spectra it is possible to deconvolve the IC spectra in the different ion specie contributions and ion charge states. The deconvolution process is checked by using the Coulomb-Boltzmann-shifted (CBS) function giving as parameters the relative ion yields, the equivalent plasma temperature (kT) and the equivalent acceleration shift voltage (Vo), as described in previously articles (Torrisi *et al*., 2002).

The comparison between CBS theory and measurements demonstrates that a very good agreement occurs at laser intensities on the order of 10^8-10^{11} W/cm^2. At higher intensities it can be applied but more difficulties arise due to the strong temperature and density gradients which induce emission of different ion groups (Torrisi *et al*., 2006).

Due to the statistical data, measurement errors, indeterminations, reproducibility of the laser pulse and statistical error propagation afflict the temperature, density, equivalent acceleration voltage and the ion kinetic energy evaluations. As a first approximation the total errors on the given values can reach also the 40–50%.

3. RESULTS

The number of protons ejected from the target can be measured in different ways. In the case of CH_2 target and for high laser intensities it can be given by using the crater volume measured with high resolution by a surface profiler, as reported in our previous articles (Torrisi *et al*., 2008). At the used laser intensity the ablation yield is of about 10^{16} CH_2 molecules/pulse, thus, assuming the fractional ionization to be about 100%, the proton emission can reach 2×10^{16} ions/pulse.

In the case of metals, due to the higher absorption coefficient of free electrons, the ablation yield, at the first laser shot on the free surface, may reach about 10^{17} atoms/pulse. At the successive laser shots the ablation yield decreases due to the not flat surface of the ablated target and to the focusing loss with the crater depth. From the experimental results it is possible to evaluate the energy conversion efficiency from laser pulse to the total energy transferred to protons; in the case of CH_2 ablation, this efficiency if on the order of 13%. This estimation is performed assuming that the laser pulse energy (800 mJ) is transferred to the total number of molecules ejected from the laser crater (10^{16} CH_2 molecules), which 2/3 is constituted by protons, and assuming that the mean proton energy is about 100 eV. This evaluation represents an approximated value because for the exact efficiency conversion value it is necessary to consider also the proton energy distribution (that has a Boltzmann shape), the proton angular distribution (that has a main emission within ± 45%) and the proton recombination effect.

Figure 2 shows four typical IC-TOF spectra obtained irradiating (single shot at 800 mJ and 1.8×10^{10} W/cm^2 pulse intensity) a target of CH2-bulk (a) and Ti (b), Al (c) and Au (d) targets, the last three covered by 50 μm CH_2 thin film.

Spectra show a fast little peak, due to the proton detection at time values lower than about 5 μs, followed by a slower and higher peak, due to the multi-ionized bulk ion species. The mean proton energy, valuable from the fast peak, is about 90 eV, 155 eV, 165 eV, and 195 eV for CH_2, Ti, Al, and Au plasmas, respectively.

IEA spectra permitted to measure the number of charge states in the experimental used conditions of laser-target interaction. As an example, Figure 3 shows an IEA spectrum (top) reporting the seven charge states measured in the Ti target and the corresponding IC spectrum (bottom). The IEA spectrum shows the start photo-peak, the seven peaks due to the different Ti ion charge states and the peaks due to the presence of absorbed hydrogen and oxygen (five charge states) at the target surface. The IC spectrum shows the integral of all detected ions. The measured charge states for the elements analyzed in the other laser irradiated targets were 4, 5, 10 for the C, Al, and Au atoms, respectively.

Taking into account the maximum number of charge states measured through IEA and of the ionization potentials of the irradiated target elements, it was possible to evince the possible deconvolution spectra of the integral spectrum of the de-

https://doi.org/10.1017/S0263034610000728 Published online by Cambridge University Press

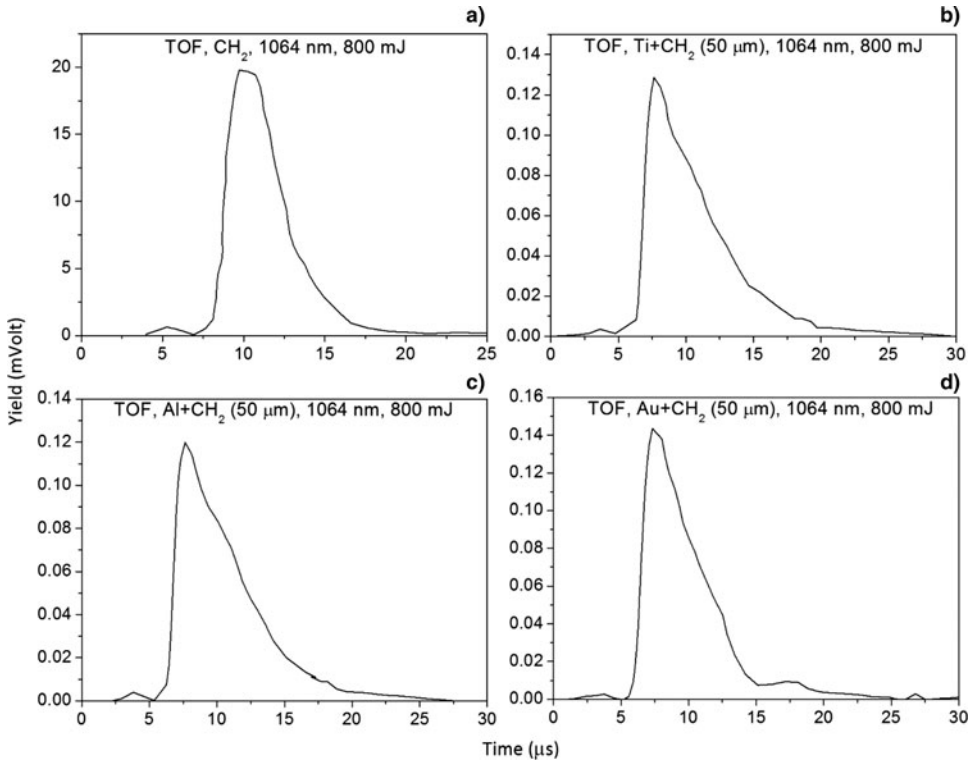

Fig. 2. Four typical IC-TOF spectra obtained irradiating a target of CH_2-bulk (**a**), Ti covered by 50 μm CH_2 (**b**), Al covered by 50 μm CH_2 (**c**) and Au covered by 50 μm CH_2 (**d**).

tected ions. As an example, based on the IEA charge state spectra, Figures 4a–4d show the CBS ion deconvolution spectra for the integral ion signals (dots) presented in Figure 2. The mathematical process was developed by applying the CBS function with the ion equivalent temperature, kT, and acceleration voltage, V_0, as input parameters. The equivalent ion temperature best fit was obtained with 10 eV (a), 19 eV (b), 21 eV (c), and 25 eV (d) for CH_2, Ti, Al and Au plasmas, respectively. The equivalent ion acceleration voltage best fit was obtained with the values of 67 V (a), 110 V (b), 120 V (c), and 135 V (d), for the four cases, respectively. The insets of the four figures report the ionization potentials *versus* the number of charge states, indicating that the number of charge states depends on the mean hydrogen ions energy, i.e., indicating that when the ionization potential is higher than the mean hydrogen ions energy the ionization doesn't occurs.

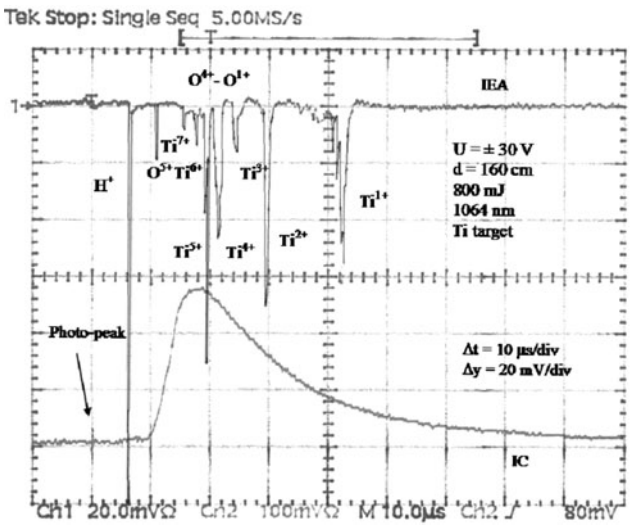

Fig. 3. Typical IEA spectrum relative to the seven charge states measured in the Ti targets and to the presence of absorbed hydrogen and oxygen at the target surface.

At the used laser intensity, of the order of 10^{10} W/cm^2, the equivalent plasma temperature relative to the "core" position is approximately the same for the different ion species. The different ion kinetic energy is due mainly to their different charge state and to the Coulomb effects occurring inside the plasma. However, at high laser intensity, above 10^{13} W/cm^2, the IEA spectra show ion energy distributions that cannot be fitted by a single temperature value, as reported in our previously paper (Torrisi *et al.*, 2006). In these cases higher temperature gradients are present and the IC spectra need to be deconvolved by using different temperature values for different ion groups. Generally increasing the ion charge state the equivalent temperature increases and ions are emitted in different groups of different temperatures. Of course by changing the target composition, at the same laser intensity, the plasma temperature is different, as reported in the results shown in Figure 4.

Ions are accelerated through three processes, the thermal interactions, the adiabatic plasma expansion in vacuum and

https://doi.org/10.1017/S0263034610000728 Published online by Cambridge University Press

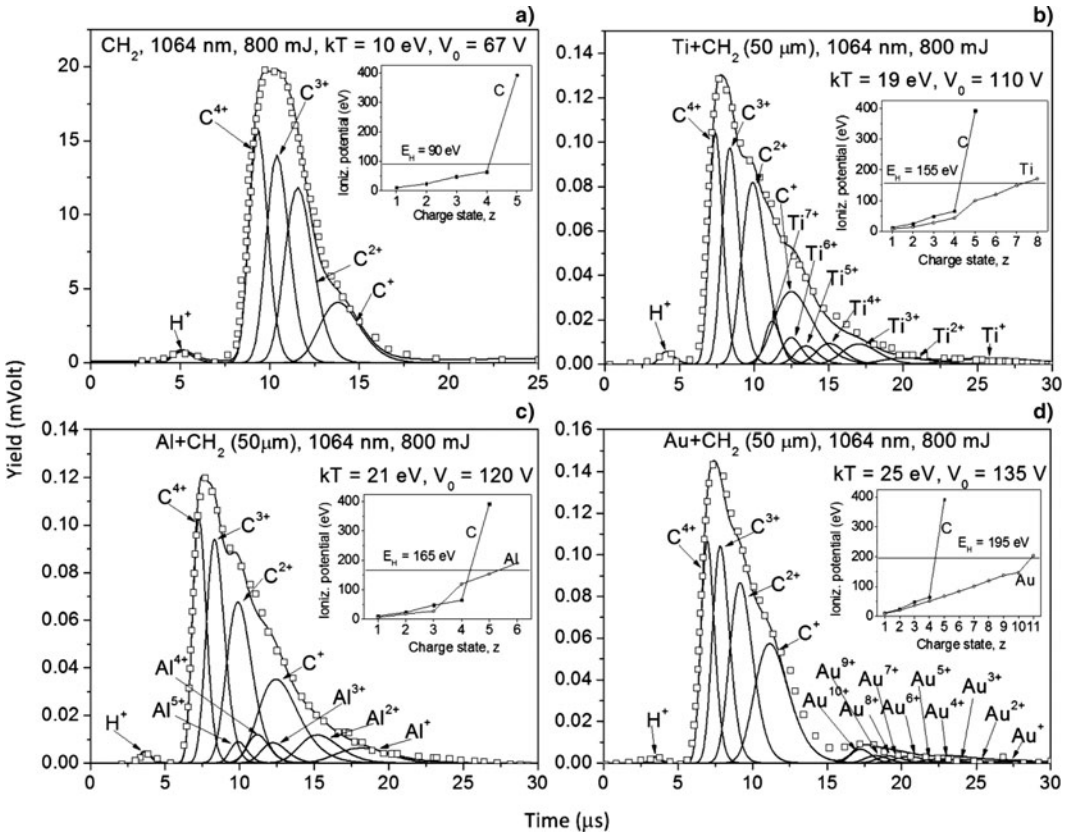

Fig. 4. Based on the IEA charge states spectra, the figure reports the CBS ion deconvolution spectra for the integral ion signals (dots) presented in Fig. 2.

the Coulomb interactions, due to the acceleration in the electric field developed in the charge separation inside the non-equilibrium plasma. Thus, the total ion energy assumed along the normal to the target surface direction is:

$$E_{tot} = E_T + E_k + E_C = \frac{3}{2}kT + \frac{\gamma}{2}kT + ezV_0. \qquad (2)$$

At high charge states and at high pulse intensity, at which high voltage V_0 can be developed, the Coulomb acceleration becomes predominant with respect to the thermal ones. Figure 4a indicates that for measured proton energy of 90 eV the corresponding plasma temperature kT is only about 10 eV while the eV_0 value is 67 eV. The inset of the same figure indicates that 90 eV proton energy is sufficient to induce ionization in carbon atoms up to fourth charge state. This consideration comes from the comparison between the experimental results and the theoretical ionization potential of the elements. The equivalent plasma temperature is relative to the ion species but assuming the condition to be in near local thermal equilibrium (NLTE), it is possible to assume that this temperature is approximately the same of the electronic one (Ti ~ Te).

A summary of the above described results is reported in the three plots of Figure 5. The proton kinetic energy (a), the equivalent ion temperature (b), and the equivalent acceleration voltage (c) are reported as a function of the electrical conductivity of the metallic substrate target. These three parameters increase with the electrical conductivity, i.e., with the density of free electron states in the target. Increasing the free electron density the laser absorption coefficient increases and the plasma becomes hotter. Thus, in order to obtain higher proton energy, it is better to use an Au target, with the higher free electron density and electrical conductivity, covered by a thin polyethylene film. This target structure injecting electrons in the plasma increases the charge not-equilibrium of the plasma permitting to accelerate protons up to about 200 eV.

In order to increase the proton kinetic energy and yield emission, measurements by changing the thickness of the CH_2 thin film covering the metal target substrate were performed. A lot of results are reported in Figure 6 relatively to the laser irradiation of Ti targets covered by different films of polyethylene, from 10 μm (a) to 30 μm (b), and to 50 μm (c). The experimental spectra (dots) are CBS deconvolved in the various ion contributions due to the different Ti, C, and H ion charge states. Results demonstrate that increasing the polyethylene film thickness the proton energy, the equivalent ion temperature and the ion acceleration voltage decrease, while the proton yield increases, as reported in Figure 7. This effect can be justified by the low laser absorption in the thin polyethylene film, by the transmitted laser shot interaction with the metallic surface, by the

https://doi.org/10.1017/S0263034610000728 Published online by Cambridge University Press

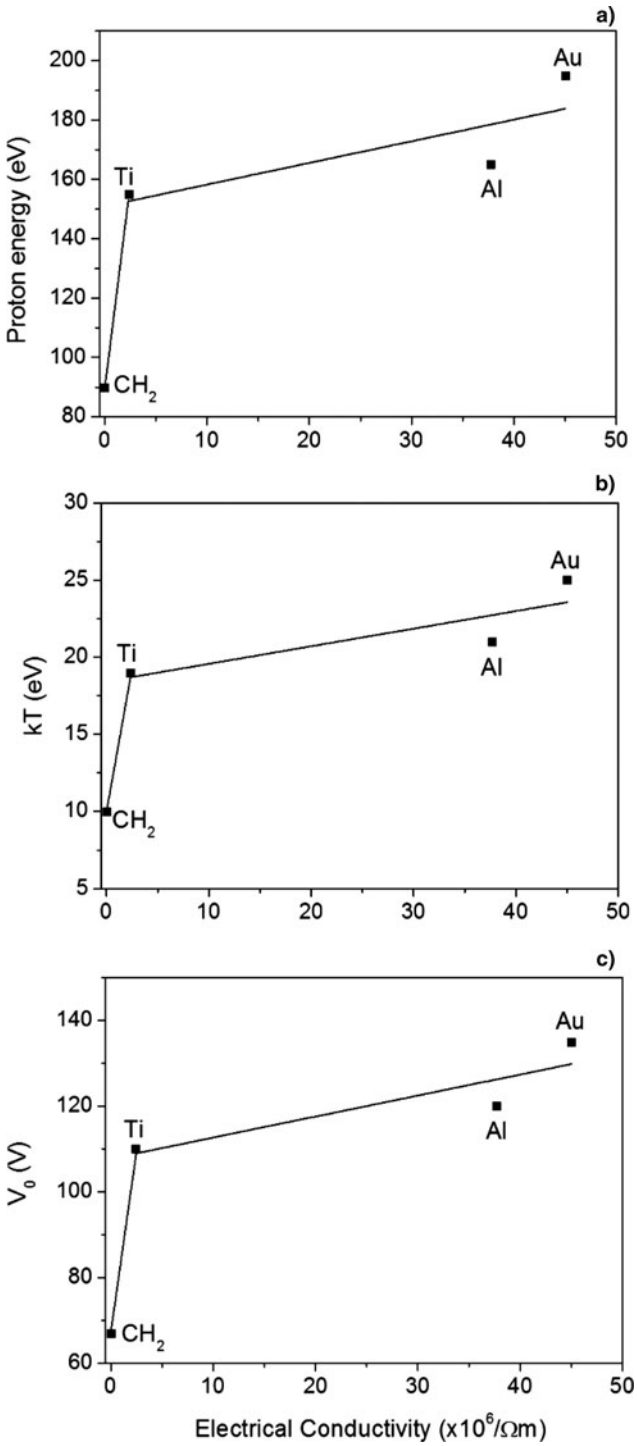

Fig. 5. The proton kinetic energy (**a**), the equivalent ion temperature (**b**) and the equivalent acceleration voltage (**c**) as a function of the electrical conductivity of the metallic substrate target.

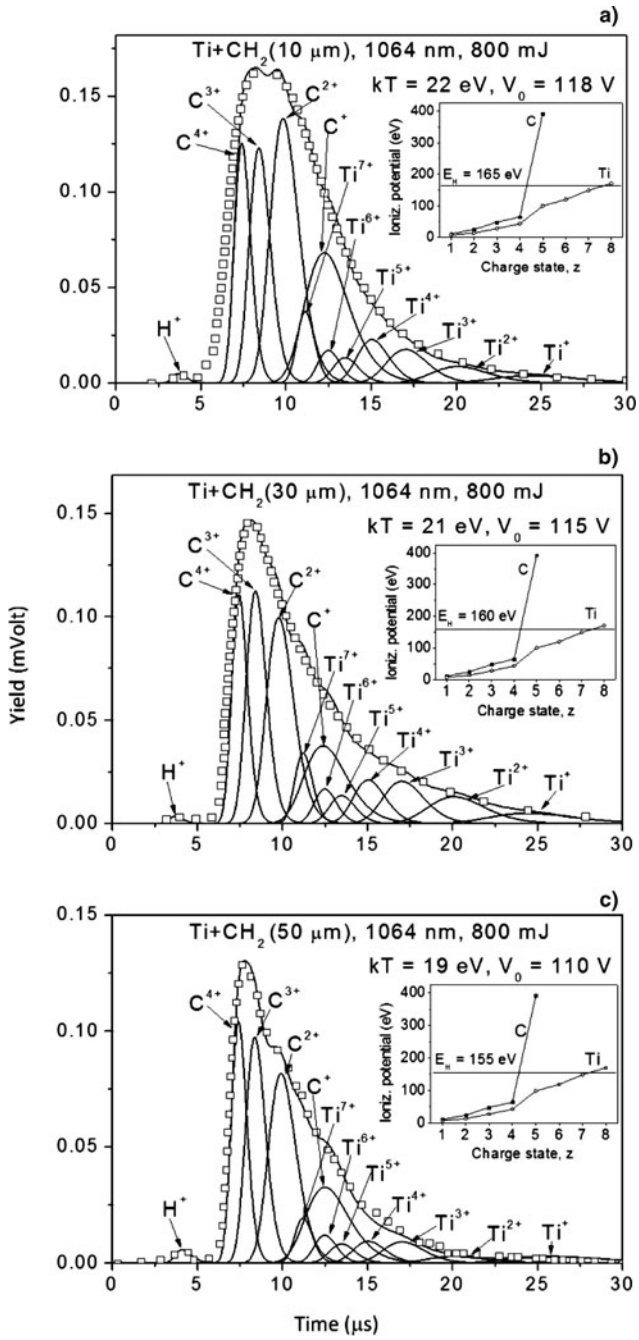

Fig. 6. IC spectra relative to laser irradiation of Ti targets covered by 10 μm (**a**), 30 μm (**b**), and 50 μm (**c**) polyethylene film and relative CBS ion deconvolution spectra.

consequent plasma formation at the metal-polymer interface and by the successive explosion of the polymeric film with release of accelerated carbon, hydrogen and metal ions.

Polyethylene is partially transparent to the used laser irradiation, thus a component of the laser photons are transmitted from polyethylene up to the back metal. From this metal surface electrons are generated and a component can participate to the laser generated plasma increasing the electron density. This effect occurs only for thin polymeric films. In thick film, of course, this phenomenon doesn't occur and consequently the electron density of the plasma is lower due to the low electron density of the polymer compound. Plasma is generated both from the thin polymeric film and from the first layers of the metal surface. A possible explanation of the mechanisms occurring in the target is the following: the faster process consists in the IR light transmission from the

https://doi.org/10.1017/S0263034610000728 Published online by Cambridge University Press

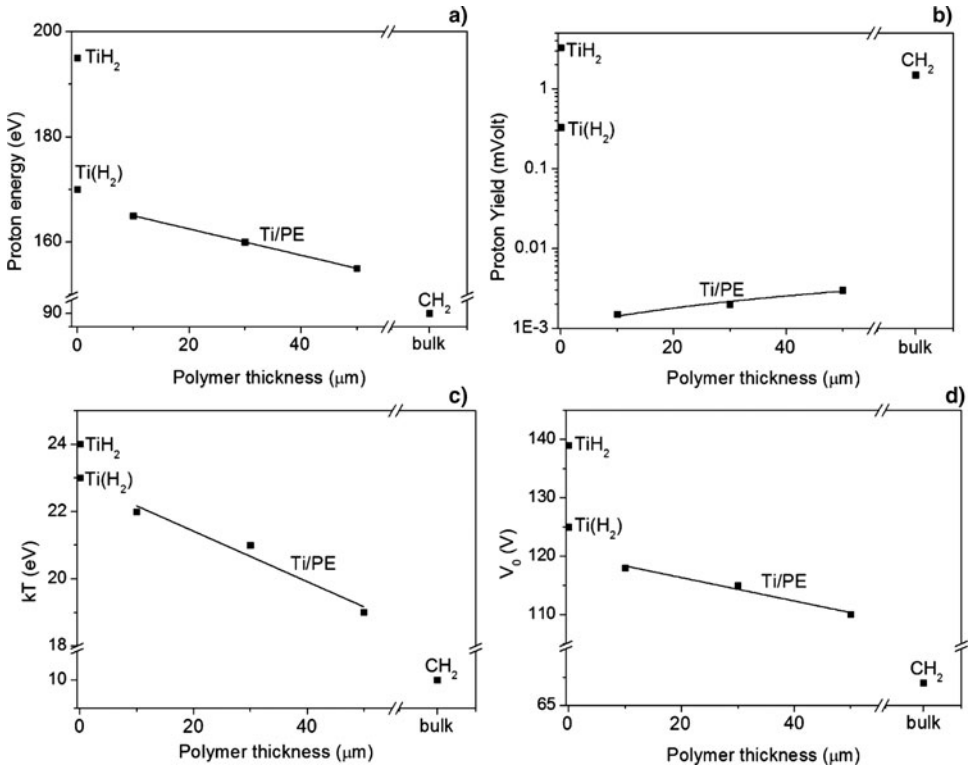

Fig. 7. The proton energy (**a**), the proton yield (**b**), the plasma temperature kT (**c**) and the acceleration voltage Vo (**d**) as a function of the polymer thin film thickness covering the Ti target substrate, and relatively to the measurements in the TiH_2, $Ti(H_2)$ and CH_2 bulk targets.

polymer film to the metal surface, in the metal reflection towards the covering polymer and in the high metal absorption due to the free electrons of the first surface layers. The successive temporal process consists in the formation of a high density of free energetic electrons, more of which are injected in the polymer, responsible of ionizations generated inside the metal and inside the covering polymer. Successively to the electron emission from the metal towards the polymer and from the polymer towards the vacuum, a high density of positive ions occurs. Coulomb explosions can take place with emission of energetic ions from the metals and from the polymer. Within a temporal scale of the order of the laser pulse duration (9 ns) it is possible to assume that the plasma originates before from the metal and after from the polymer. During the just after the laser pulse a plasma containing electrons and ions coming from the metals and from the polymer is generated in expansion conditions from the laser crater.

Thus Figure 5 reports as an indication of the dependence effects on the free electron density in the metal substrate. This substrate, in fact, participates to the electron density of the plasma, and of the thin polymeric film that promotes the ion acceleration only at very low thickness. Of course, the thin film is partially transparent to the used laser radiation and below about 50 μm thickness the plasma is influenced by the below metal surface.

To increase the proton stream amount it is better to use thick films because more hydrogen can be ejected. However, this effect decreases the proton energy proportionally to the film thickness, due to the decrease of the transmitted laser energy impinging on the metallic substrate. From this point of view the proton energy increase can be obtained through the use of thin films or by using absorbed hydrogen in the metallic target bulk or hydrogenated metallic targets, as the titanium hydrate sheets, TiH_2, employed in these investigations. Figure 7 shows also, for comparison, the measurement results obtained irradiating other hydrogenated bulk targets.

Figure 8 reports two typical IC spectra with relative CBS deconvolution of the involved ion species. The first spectrum is relative to the Ti bulk metal with absorbed hydrogen (a) while the second one is relative to the TiH_2 bulk metal (b). The relative deconvolution spectra are reported in Fig. 8c and 8d, respectively. In these two cases the mean proton energy assumes the value of 170 eV and 195 eV. For comparison, the measurements performed with the thick targets of TiH_2, $Ti(H_2)$ and CH_2 are reported in Figure 7.

Moreover, our investigations, performed not only at single laser shot but also with a repetitive laser pulse irradiation from 1 to 10 Hz, demonstrated that in the case of the absorbed hydrogen in Ti ($Ti(H_2)$-target) the proton amount is high only at the first laser shot and it decreases at the successive ones (in the same spot position), due to the thermal effects that induce hydrogen diffusion and degassing from the surface. In the case of titanium hydrate target, TiH_2, the hydrogen amount is very high because its concentration is higher with respect to the same titanium and its proton

https://doi.org/10.1017/S0263034610000728 Published online by Cambridge University Press

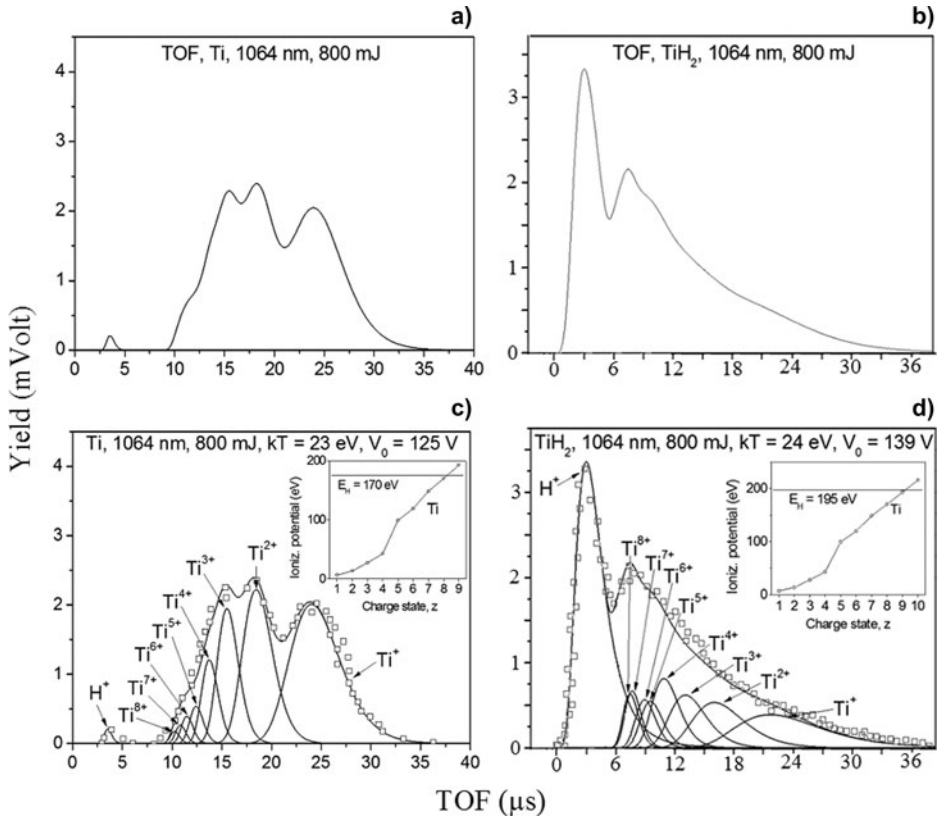

Fig. 8. Comparison between the IC peaks detected in pure Ti (**a**) and in TiH_2 (**b**) targets ablated in the same experimental conditions and relative CBS deconvolution processes (**c**, **d**).

emission remains high also for repetitive laser shots given in the same spot position.

The maximum proton yield emission is obtained by using a bulk hydrogenated target. Three cases permit to generate an high number of proton emission: the titanium hydrate (TiH_2), the titanium bulk with absorbed hydrogen ($Ti(H_2)$), and the thick polyethylene target (CH_2). In these three cases the TOF proton peak was evaluated 3.3 mV, 0.33 mV, and 1.5 mV, respectively. In order to generate protons with a high repetitive laser pulses the TiH_2 and the CH_2 targets are suitable because protons are generated in a reproducible way, while the $Ti(H_2)$ target is not adapt because the proton amount decreases with the number of laser shots, due to hydrogen degassing induced by the laser heating.

4. DISCUSSION AND CONCLUSIONS

The laser ion source (LIS) of protons and the post acceleration process can result useful for some experiments. At INFN-LNS of Catania, for instance, 30–80 kV post acceleration voltage is employed to accelerate protons and other ions, at energies proportional to 30–80 keV depending on their charge state. The ion beams, monochromatic for protons and multi-energetic for other ions, can be obtained by using 10–30 Hz laser repetition rate and with a proton flux of the order of 10^{10}/pulse, corresponding to a current of about 20–50 nA. Such LIS coupled to post-acceleration method is prepared in order to accelerate deuteron beams to induce D-D nuclear fusion reactions by deuterium ions with deutered secondary targets interactions. The experiment permits to generate 2.5 MeV neutrons and 3 MeV protons thank to the high nuclear cross-section obtainable at the low deuteron energy. The method of neutron and proton generation from the induced D-D fusion is interesting because very economical, well controllable and useful for many astrophysical investigations.

The ns laser pulse intensities of the order of 10^{10} W/cm^2 are sufficient to produce hot plasmas, with duration comparable with the laser pulse (9 ns) and temperature ranging between about 10 and 25 eV. The ion emission can be investigated on line by using IC and IEA detectors in TOF configuration and by applying the CBS distribution function, in order to evaluate the ion emission contribution in terms of specie and charge state. In particular the proton emission can be implemented by using hydrogenated thick target that can be prepared through thin polymeric films covering the metallic surface, by using thick polymers, by using the absorbed hydrogen in the metallic surface or by using specific hydrated compounds.

The proton kinetic energy and amount are a function of the target composition and of the laser shot parameters used in this experiment.

https://doi.org/10.1017/S0263034610000728 Published online by Cambridge University Press

The maximum equivalent plasma temperature is reached by using a thin polyethylene film covering the high electrical conductive gold substrate or the TiH_2 metallic compound as target, which permit to obtain 25 eV and 24 eV equivalent plasma temperature, respectively. These values indicate that the thermal ion energy should be $E_t = 3\ kT/2 \sim 37$ eV and that the gas expansion velocity confers to the ions an energy of about $E_k = \gamma kT/2 \sim 21$ eV, being γ the adiabatic coefficient of the mono-atomic species ($\gamma = 1.67$). In these two cases, the total proton energy, E_p, has the maximum value of about 195 eV. Thus, it is possible to evaluate the Coulomb energy contribution, E_c, acquired by the protons in the high electric field generated inside the plasma, given by the difference:

$$Ec = E_p - E_t - E_k = (195 - 37 - 21)eV = 137eV \qquad (3)$$

This consideration demonstrates that the equivalent acceleration voltage, Vo, at which proton are submitted is of about 137 V, in good agreement with the value used in the fit deconvolution of the IC spectra obtained by using the CBS function distribution of Eq. (1) and reported in Figures 4d, 5c, and 8d, respectively.

Polyethylene has not free electrons and it, as bulk target, doesn't permit to accelerate ions above 90 eV (see Fig. 5a). Thus, the high proton energy of 195 eV can be explained on the base of the high conductive metallic substrate that acts as an electron injector in the plasma increasing the electron density. Such electrons increase the charge distribution in the separation space between the electron and ion clouds generated on the target surface, i.e., increase the electric field of the plasma responsible of the high Coulomb ion acceleration (Torrisi & Gammino, 2006).

In conclusion, at the used laser pulse intensity of the order of 10^{10} W/cm^2, in order to generate high energy, high amount of proton emission and repetitive proton ejection from the plasma, the best of our targets was the TiH_2 one.

REFERENCES

Torrisi, L., Cavallaro, S., Giuffrida, L., Gammino, S. & Andò, L. (2010). Ti post-ion acceleration from laser ion source. *Rad. Effects & Defects in Solids: Incorporating Plasma Science & Plasma Technology*, Vol. **165**, No. 6, 1–12.

Badziak, J., Kasperczuk, A., Parys, P., Pisarczyk, T., Rosiński, M., Ryć, L., Wolowski, J., Suchańska, R., Krása, J., Krousky, E., Láska, L., Mašek, K., Pfeifer, M., Rohlena, K., Skala, J., Ullschmied, J., Dhareshwar, L.J., Földes, I.B., Suta, T., Borrielli, A., Mezzasalma, A., Torrisi, L. & Pisarczyk, P. (2008). The effect of high-*Z* dopant on laser-driven acceleration of a thin plastic target. *Appl. Phys. Lett.* **92**, 211 502.

Torrisi, L., Margarone, D., Gammino, S. & Andò, L. (2007). Ion energy increase in laser-generated plasma expanding through axial magnetic field trap. *Laser and part. Beams* **25** (3), 435.

Laska, L., Jungwirth, K., Krasa, J., Pfeifer, M., Rohlena, K., Ullschmied, J., Badziak, J., Parys, P., Wolowski, J., Gammino, S., Torrisi, L. & Boody, F.P. (2005). Charge-state and energy enhancement of laser-produced ions due to nonlinear processes in preformed plasma. *Appl. Phys. Lett.* **86**, 081502.

Clark, E.L., Krushelnick, K., Zepf, M., Beg, F.N., Tarakis, M., Machacek, A., Santala, M.I.K., Watts, I., Norreys, P.A. & Dangor, A.E. (2000). Energetic Heavy-Ion and Proton Generation from Ultraintense Laser-Plasma Interactions with Solids. *Phys. Rev. Lett.* **85**(8), 1654.

Woryna, E., Parys, P., Wolowski, J. & Mroz, W. (1996). Corpuscular diagnostics and processing methods applied in investigations of laser-produced plasma as a source of highly ionized ions *Laser Part. Beams* **14**, 293.

Torrisi, L., Caridi, F., Margarone, D. & Giuffrida, L. (2008). Nickel plasma produced by 532-nm and 1064 nm pulsed laser ablation. *Plasma Physics Reports*, Vol. **34**, No. 7, 547.

Torrisi, L., Gammino, S., Andò, L. & Laska, L. (2002). Tantalum ions produced by 1064 nm pulsed laser irradiation. *J. Appl. Phys.* **91**(5), 4685.

Caridi, F., Torrisi, L. & Giuffrida, L. (2010). Time-of-flight and UV spectroscopy characterization of laser-generated plasma. *Nucl. Instr. and Meth. B* **268**, 499.

Torrisi, L., Gammino, S., Andó, L., Laska, L., Krasa, J., Rohlena, K., Ullschmied, J., Wolowski, J., Badziak, J. & Parys, P. (2006). Equivalent ion temperature in Ta plasma produced by high energy laser ablation. *J. Appl. Phys.* **99**, 083301.

Torrisi, L., Lorusso, A., Nassisi, V. & Picciotto, A. (2008). Characterization of laser ablation of polymethylmethacrylate at different laser wavelengths. *Radiation Effects & Defects in Solids* Vol. **163** (3), 179–187.

Torrisi, L. & Gammino, S. (2006). Method for the calculation of electrical field in laser-generated plasma for ion stream production. *Rev. Sci. Instr.* **77**, 03B707.

https://doi.org/10.1017/S0263034610000728 Published online by Cambridge University Press